Electronic supplementary information for

Polymer-functionalised Polymer Nanoparticles and their Behaviour in Suspensions

*Waraporn Wichaita,[a,b] Young-Gon Kim,[a] Pramuan Tangboriboonrat,[b] Héloïse Thérien-Aubin[a]**

[a] Max Planck Institute for Polymer Research, Ackermannweg 10, 55128, Mainz, Germany

[b] Department of Chemistry, Faculty of Science, Mahidol University, Rama 6 Road, Phyathai, Bangkok 10400, Thailand

Experimental section

Material

Styrene, methylacrylate and divinylbenzene were purified on a column of basic aluminum oxide. Methacryloyl chloride was purified by distillation under reduced pressure. 2,2'-azobis(2-methylbutyronitrile) was recrystallized in MeOH. All other chemical reagents, 2-hydroxyethyl disulfide, 2-bromoisobutyrylbromide, trimethylamine. Cu(II) chloride, ascorbic acid, polydimethylsiloxane (5 cSt), *N,N,N′,N″,N″*-pentamethyldiethylenetriamine, sodium dodecyl sulfate, cetyltrimethylammonium chloride, hexadecane, DL-dithiothreitol, 1,8-diazabicyclo[5.4.0]indec-7-ene, hydrochloric acid, ammonium chloride, sodium hydrogen carbonate, sodium chloride, ethyl acetate, dichloromethane, *N,N'*-dimethylformamide, anisole, tetrahydrofuran, hexane, diethylether, and methanol, were used as received.

Synthesis of the ATRP inimer: 2-((2-(3-Methyl-2-oxobut-3-en-1yl)xy)ethyl)disulfanyl)ethyl 2-bromo-2-methylpropanoate (MA-SS-Br)

MA-SS-Br was synthesized via a 2-step esterification (Figure S1).[1] Briefly, 600 mL of DCM was added to a round bottom flask and cooled to 0°C. Under stirring, 23.8 g of (2-hydroxyethyl) disulfide (1.1 eq) and 67.8 mL of trimethylamine (2.6 eq) was added. Then, 21.6 mL of 2-bromoisobutyryl bromide (1.0 eq) was slowly added to the reaction mixture using a

syringe pump (15 ml/h). The reaction mixture was left stirring overnight at room temperature and was then filtered. The organic phase was then washed by extraction with sequentially 1 M HCl (3 X 400 mL), sat. $NaHCO_3$ (3 X 600 mL) and sat. NaCl (3 X 600 mL). The organic phase was then dried with $MgSO_4$ and evaporated under reduced pressure. The resulting oil was purified by silica column chromatography (hexane:EtOAc = 6:4, R_f = 0.56). ^{1}H-NMR spectroscopy (300 MHz, $CDCl_3$): chemical shift (δ/ppm) of 4.46 (t, 2H), 3.91 (t, 2H), 2.99 (t, 2H), 2.90 (t, 2H), 1.96 (s, 6H) (Figure S1(i)). The resulting 2-((2-hydroxyethyl)disulfanyl)ethyl-2-bromo-2-methylpropanoate (HO-SS-Br, 16g, 1.0 eq) was dissolved in 144 mL of DCM, 15 ml of trimethylamine (2.5 eq) was added to the solution which was then cooled to 0°C. Then, 14.26 mL of freshly distilled methacryloyl chloride (3.0 eq) was added dropwise to the reaction mixture and the reaction was left stirring overnight at room temperature. The precipitate was filtered off and the solution was washed by extraction with 1 M HCl (3 X 360 mL) and sat.$NaHCO_3$ (3 X 430 mL). After drying the organic phase with $MgSO_4$, the solvent was removed and the product was purified with a silica column (hexane:EtOAc = 6:4, R_f = 0.2). To eliminate remaining impurities, the mixture was purified with a second column (hexane:diethyl ether = 9:1, R_f = 0.46) resulting in the pure MA-SS-Br. ^{1}H-NMR spectroscopy (300 MHz, $CDCl_3$): δ/ppm of 6.07 (m, 1H), 5.53 (m, 1H), 4.36 (m, 4H), 2.91 (m, 4H), 1.87 (m, 9H) (Figure S1(ii)).

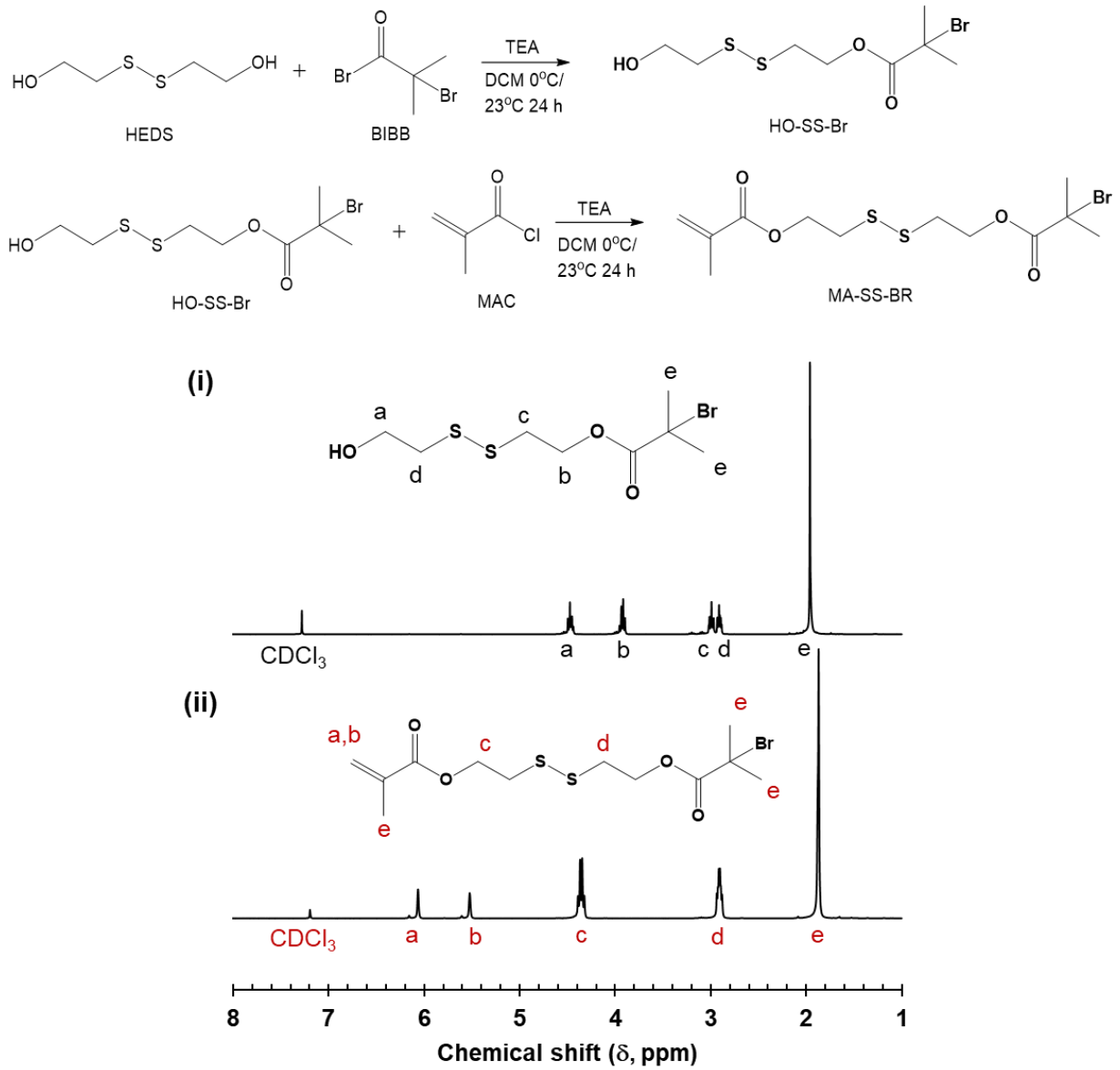

Figure S1. Synthesis and characterization of the ATRP inimer containing a disulfide bond (MA-SS-Br). ^{1}H-NMR spectra of (i) 2-((2-Hydroxyethyl)disulfanyl)ethyl-2-Bromo-2-methylpropanoate and (ii) 2-((2-(3-Methyl-2-oxobut-3-en-1yl)xy)ethyl)disulfanyl)ethyl 2-bromo-2-methylpropanoate.

Nanoparticle characterization

The size of particles was characterized by DLS (Malvern Nano-S90) using water and anisole as solvents.

Table S1. Flory-Huggins interaction parameters

Solvent	Solvent quality (χ)×	
	PS	PMA
Anisole	0.18	0.25
DMSO	1.40	0.30
Water	3.13	2.33

× Calculated from the Hansen solubility parameters[2]

FTIR spectra were recorded on a FTIR spectrophotometer (PerkinElmer Frontier) equipped with a diamond ATR crystal between 4000−600 cm^{-1}. ^{1}H-NMR spectra were recorded on a Bruker AMX-300 NMR instrument operating at 300.1 MHz. Size exclusion chromatography (SEC) (Agilent Technologies 1260 Infinity) was measured in THF using a series of linear polystyrene as calibration. To prepare samples for SEM, suspensions of NPs in DCM were spin-casted on silicon wafers. SEM was performed with an acceleration voltage of 0.182 kV on a Hitachi SU8000 microscope.

Table S2. Library of PS@PMA nanoparticles

Sample	Initiator/MA/Cu(II)/ PDMETA/ASAC	Time (h)	*N*	M_n NMR (kDa)	SEC		Particle size (nm)		
					M_n (kDa)	Đ	Water	DMSO	Anisole
PS with high grafting density (PS_h, σ = 2.5±0.3 chains/nm²)							120	120	210
PS_h@PMA_{3k}	1/266/0.1/1.0/0.5	0.5	36	3.1	4.2	1.7	120	--	220
PS_h@PMA_{6k}	1/533/0.1/1.0/0.5	1	70	6.0	6.6	1.9	160	--	320
PS_h@PMA_{10k}	1/533/0.1/1.0/0.5	2	128	10.0	12	2.1	140	200	300
PS_h@PMA_{15k}	1/533/0.1/1.0/0.5	2.5	171	15.0	18	2.0	120	230	340
PS_h@PMA_{20k}	1/533/0.1/1.0/0.5	3	220	19.0	21	2.1	140	--	340
PS_h@PMA_{30k}	1/1066/0.1/1.0/0.5	1	406	35.0	27	2.4	140	250	390
PS_h@PMA_{40k}	1/1066/0.1/1.0/0.5	3	493	42.0	40	2.5	140	250	440
PS_h@PMA_{50k}	1/1066/0.1/1.0/0.5	6	623	54.0	44	2.0	150	320	600
PS with medium grafting density (PS_m, σ = 0.80±0.03 chains/nm²)							110	110	210
PS_m@PMA_{3k}	1/133/0.1/1.0/0.5	0.5	31	2.6	4.2	1.9	110	--	250
PS_m@PMA_{6k}	1/266/0.1/1.0/0.5	0.5	79	6.9	8.9	2.6	100	--	260
PS_m@PMA_{20k}	1/533/0.1/1.0/0.5	3	228	20.0	20	2.2	110	200	290
PS_m@PMA_{30k}	1/1066/0.1/1.0/0.5	2	349	30.0	27	2.1	120	240	330
PS_m@PMA_{40k}	1/1066/0.1/1.0/0.5	3	493	42.0	29	2.1	120	250	320
PS_m@PMA_{50k}	1/1066/0.1/1.0/0.5	4.5	593	51.0	35	2.4	130	260	340
PS with low grafting density (PS_l, σ = 0.17±0.02 chains/nm²)							100	115	210
PS_l@PMA_{3k}	1/266/0.1/1.0/0.5	0.5	44	3.8	4.2	1.8	95	--	290
PS_l@PMA_{6k}	1/533/0.1/1.0/0.5	1	99	8.5	8.0	2.1	97	--	290
PS_l@PMA_{20k}	1/533/0.1/1.0/0.5	2	267	23.0	19	2.3	95	170	300
PS_l@PMA_{30k}	1/1066/0.1/1.0/0.5	1.5	377	32.0	15	2.2	103	180	300
PS_l@PMA_{40k}	1/1066/0.1/1.0/0.5	2	474	41.0	18	2.7	107	200	300
PS_l@PMA_{50k}	1/1066/0.1/1.0/0.5	2.5	610	52.0	34	2.2	97	180	320

Controlled polymerization of methyl acrylate.

The polymerization was initiated by the addition of ascorbic acid to a mixture of methyl acrylate (0.4 mL), Cu(II)Br_2, PMDETA (Cu(II):ligand = 1:10 molar ratio), PS-SS-Br NPs (50 mg) in anisole (4 mL). The reaction mixture also contained PDMS (0.1 mL) which acted as an internal standard to study the conversion of MA by NMR spectroscopy.

At different points in time throughout the polymerization reaction, 25 µL of the reaction mixture was withdrawn, quenched, and mixed with 600 µL of $CDCl_3$ to determine the monomer conversions by ^{1}H-NMR (300 MHz, $CDCl_3$). The decrease of the MA signal (δ = 5.86 ppm (d, 1H)) was compared to the signal of PDMS (δ = 0 ppm) acting as an internal standard.

A linear variation of the monomer conversion as a function of the polymerization time, typical of controlled polymerization, was observed (Figure S2).

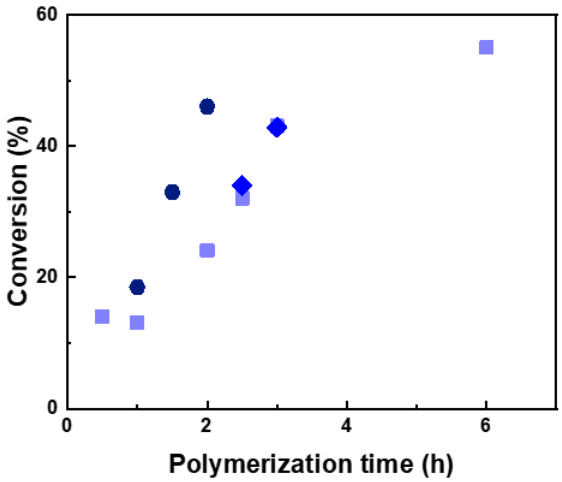

Figure S2. Monomer conversion as a function of polymerization time for the synthesis of PS@PMA using the ratio of I/MA/Cu of 1/533/0.1; (■) PS_h@PMA (2.5 chains/nm^2), (◆) PS_m@PMA (0.80 chains/nm^2) and (●) PS_l@PMA (0.17 chains/nm^2).

Composition of the PS@PMA NPs

FTIR spectra of PMA, PS NPs, PS@PMA NPs and binary mixtures of PS NPs and PMA were recorded (Figure S3). The peak at 696 cm^{-1} originating from aromatic C-H bending was used to quantify the presence of PS and the peak at 1736 cm^{-1} due to the C=O stretching was used for PMA. The area ratio observed for the PS@PMA was used to quantify the amount of PMA in each sample in comparison to a set of binary mixtures of PS NPs and free PMA.

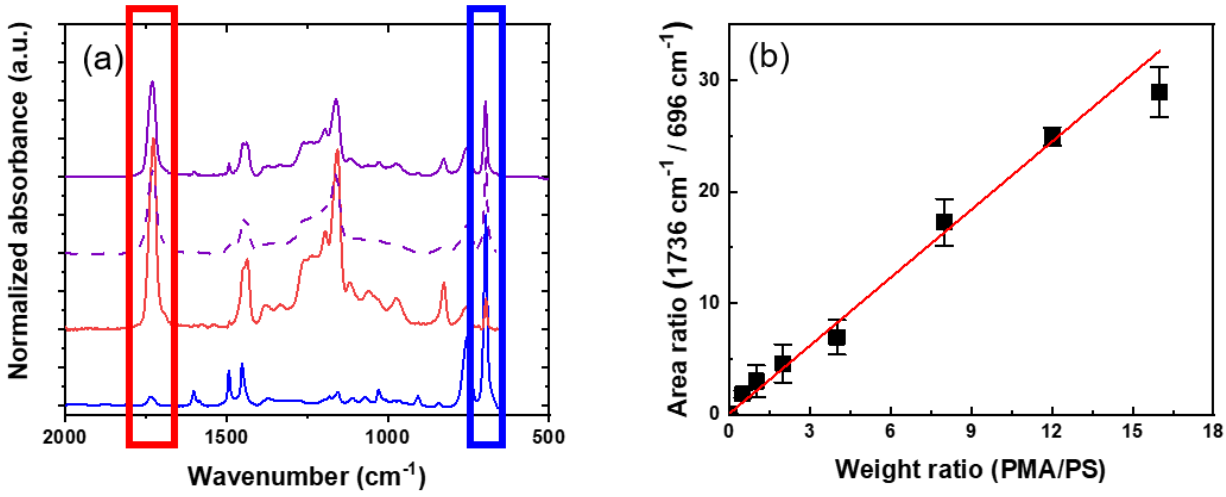

Figure S3. FTIR analysis of the PS@PMA NPs. (a) FTIR spectra of PS NPs (——), free PMA_{40k} (——), $PS_m@PMA_{20k}$ (——) and a binary mixture composed of 50 wt% of PS NPs and 50 wt% of PMA_{40k} (- - -). (b) Calibration curve used for the analysis of the PMA/PS fraction by FTIR.

Volume occupied by the nanoparticles in suspension

The size of dilute suspensions of NPs was measured by DLS, and the size of the solvated particles was used to calculate the thickness of the polymer canopy (Figure 2b, main text). The thickness of the canopy was used to show (with eq 1) that the end-tethered polymer chains were in an extended brush conformation at high grafting density and in a collapsed conformation at low grafting density (Table S3).

Table S3. The stretching parameter (α) calculated from the fitting of the variation of shell thickness and *N* (eq. 1).

Solvent	Stretching parameter (α)		
	$PS_h@PMA_x$	$PS_m@PMA_x$	$PS_l@PMA_x$
Anisole	0.8 ± 0.3	0.6 ± 0.3	0.3 ± 0.2
DMSO	0.7 ± 0.3	0.7 ± 0.3	0.3 ± 0.3
Water	0.1 ± 0.4	0.2 ± 0.5	--

However, when the volume of a solvated particle measured by DLS was used to calculate the volume occupied by the NPs in suspensions, the volume fraction obtained (ϕ_{cal}) were largely overestimated due to the possible compression and interdigitation of the polymer as the concentration of the suspension increased.

$$\phi_{cal} = \frac{V_{Swollen\ NP,\ DLS}}{V_{suspension}} \qquad \text{eq. S1}$$

Figure S4 also displays that mixing known volume of dry NPs with known volume of anisole led to no significant variation of the final volume (less than 1 vol%) suggesting that in concentrated suspension, the volume occupied by a NP was much smaller than the volume occupied by the same NP in the diluted suspensions measured by DLS. Models have been developed to estimate the effective volume fraction of hard particles in suspension, like the Krieger-Dougherty model:[3]

$$\eta_r = \left(1 - \frac{\phi_{KD}}{\phi_{max}}\right)^{-\phi_{max}[\eta]} \qquad \text{eq. S2}$$

were η_r is the relative zero-shear viscosity of the suspension and $[\eta]$ is its intrinsic viscosity, ϕ_{KD} and ϕ_{max} are respectively the effective volume fraction and the maximal volume fraction. However, this model also tends to inaccurately describe the volume fraction of suspension of soft and deformable particles (Figure S4).

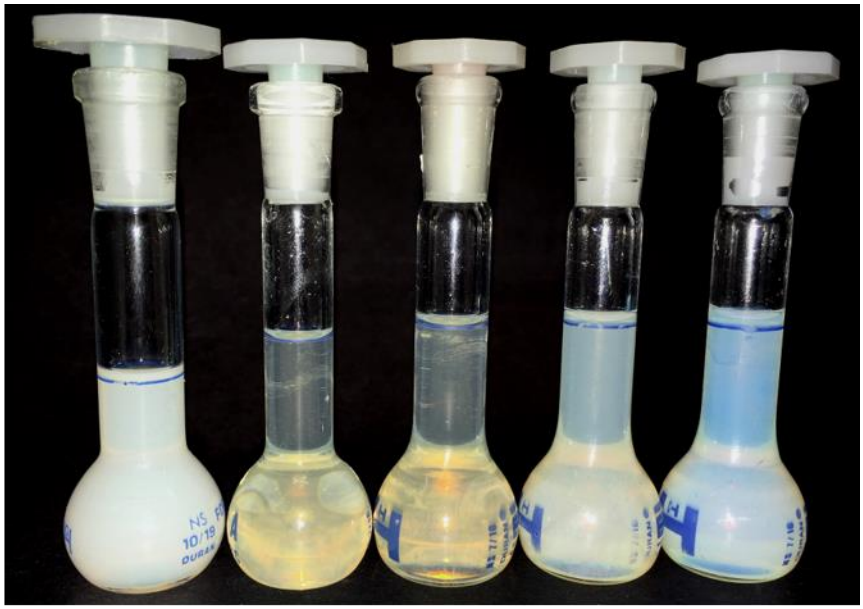

Sample	PS_h	PS_hPMA_{50k}	PS_mPMA_{50k}	PS_lPMA_{50k}	PS_lPMA_{50k}
M_{NP} (g)	0.252	0.251	0.252	0.253	0.505
M_A (g)	4.738	4.726	4.738	4.762	4.5
C_{NP} (wt%)	5.05	5.04	5.05	5.05	10.09
V_{NP} (dry) (cm^3)	0.24	0.21	0.21	0.22	0.45
V_A (mL)	4.762	4.75	4.762	4.786	4.523
# of NPs	2.52e14	2.55e13	6.77e13	2.25e14	4.49e14
R_h (nm)	104	296	168	161	161
V_{NP} (swolen) (cm^3)	1.21	2.8	1.34	3.9	7.8
V_{Total} (cm^3)	5	5	5	5	5.05
φ	0.24	0.56	0.27	0.79	1.5
φ_{KD}	0.48	0.63	0.57	0.6	0.64

Figure S4. Swelling of nanoparticles in concentrated solutions.

Rheological behavior of concentrated suspension of PS@PMA

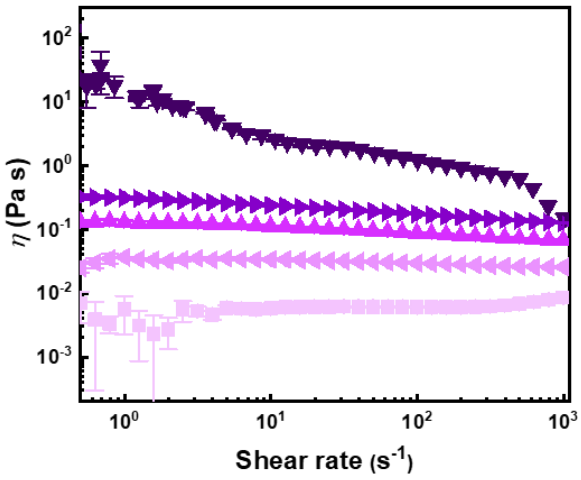

Figure S5. Influence of NPs concentration on the dynamic viscosity of suspensions of PS_h@PMA_{40k} in anisole at different concentration; (■) 2.5 wt% (ϕ_{cal} = 0.014), (◀) 3.5 wt% (ϕ_{cal} = 0.20), (▲) 5 wt% (ϕ_{cal} = 0.29), (▶) 7.5 wt% (ϕ_{cal} = 0.43) and (▼) 10 wt% (ϕ_{cal} = 0.57).

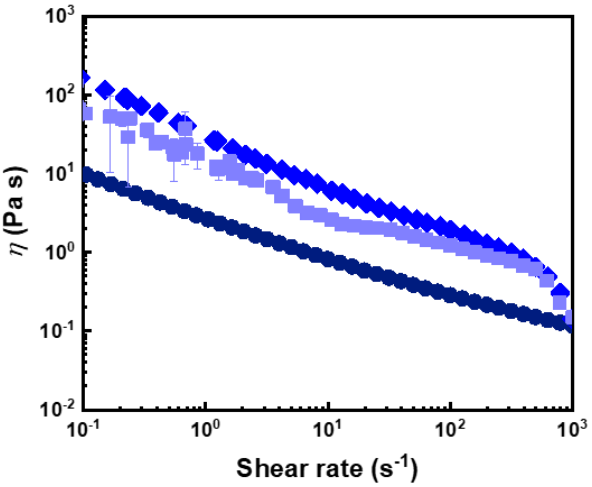

Figure S6. Continuous shear experiments of 10 wt% suspensions of PS_x@PMA_{40k} NP. (■) PS_h@PMA_{40k} , (◆) PS_m@PMA_{40k} and (●) PS_l@PMA_{40k} in anisole.

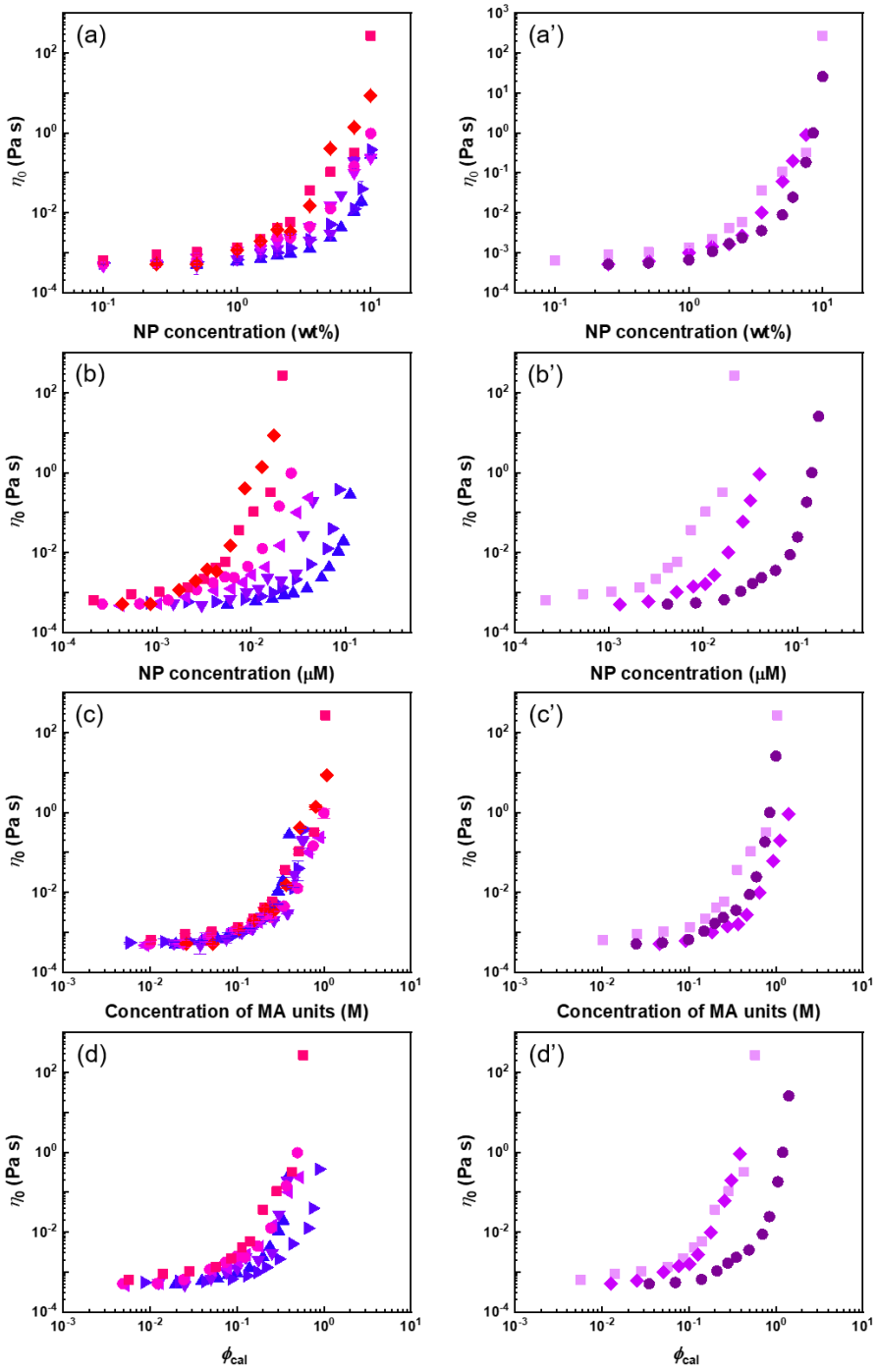

Figure S7. Zero-shear viscosities of PS@PMA NPs suspensions at different concentrations in anisole given in weight fraction of NPs (a), in molar concentration of NPs in suspension (b), in molar concentration of methyl acrylate units in the suspension (c) or in the calculate volume fraction (eq. S1) occupied by the NPs (d). For (a,b,c,d) (▲) $PS_h@PMA_{3k}$, (▶) $PS_h@PMA_{6k}$, (▼) $PS_h@PMA_{10k}$, (◀) $PS_h@PMA_{20k}$, (●) $PS_h@PMA_{30k}$, (■) $PS_h@PMA_{40k}$ and (◆) $PS_h@PMA_{50k}$ and for (a', b', c') (■) $PS_h@PMA_{40k}$, (◆) $PS_m@PMA_{40k}$ and (●) $PS_l@PMA_{40k}$.

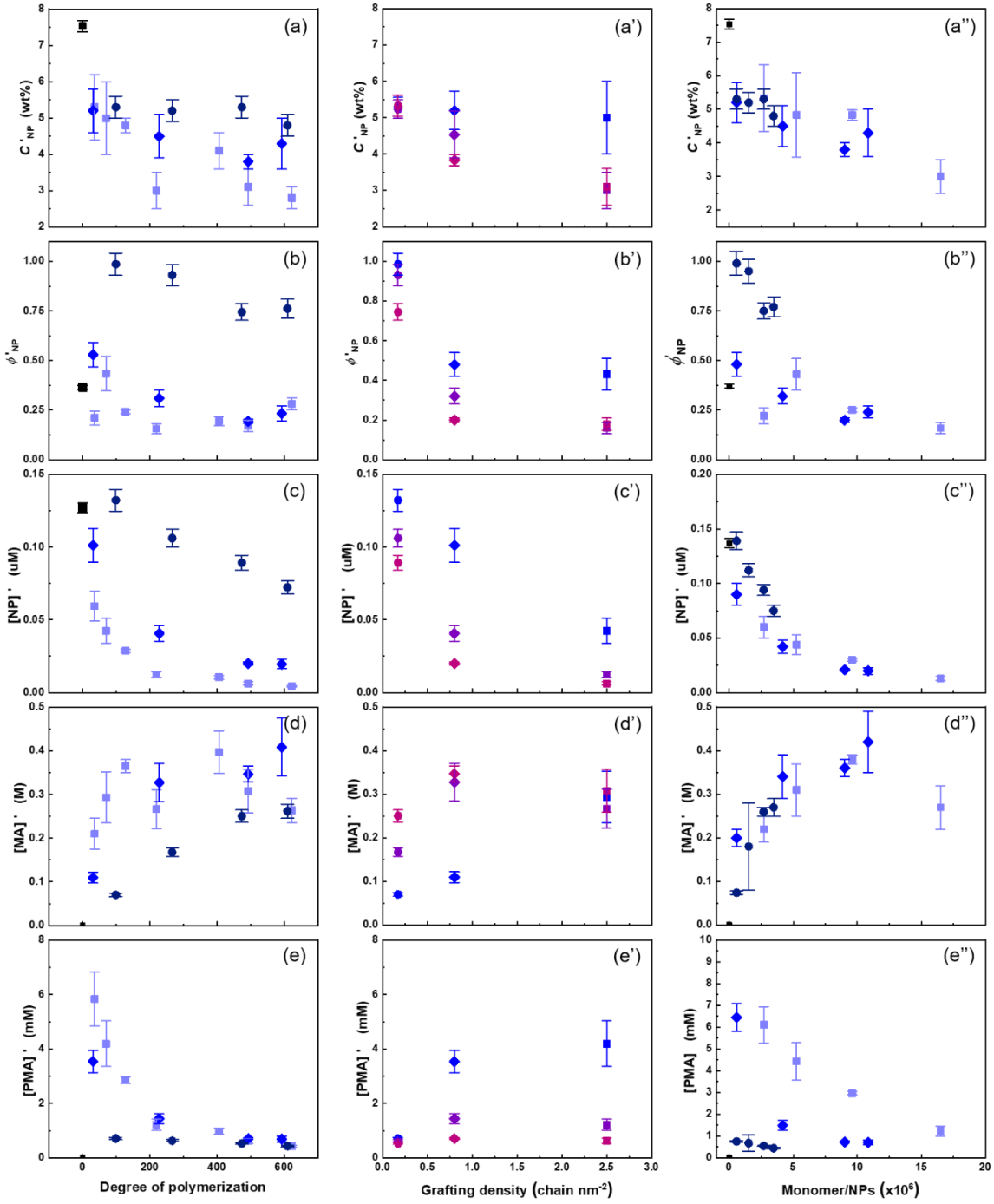

Figure S8. Variation of *C*' in anisole with the architecture of the PMA canopy. With *C*' expressed in (a) weight fraction of NPs in suspension, (b) volume fraction (eq. S1) of NPs in suspension, (c) molar concentration of NPs, (d) molar concentration of methyl acrylate units in suspension and (d) molar concentration of poly(methyl acrylate) chains in suspension. For (■) PS NPs, (■) PS_h@PMA, (◆) PS_m@PMA and (●) PS_l@PMA and (●) PS_x@PMA_{6k}, (●) PS_x@PMA_{20k} and (●) PS_x@PMA_{40k}.

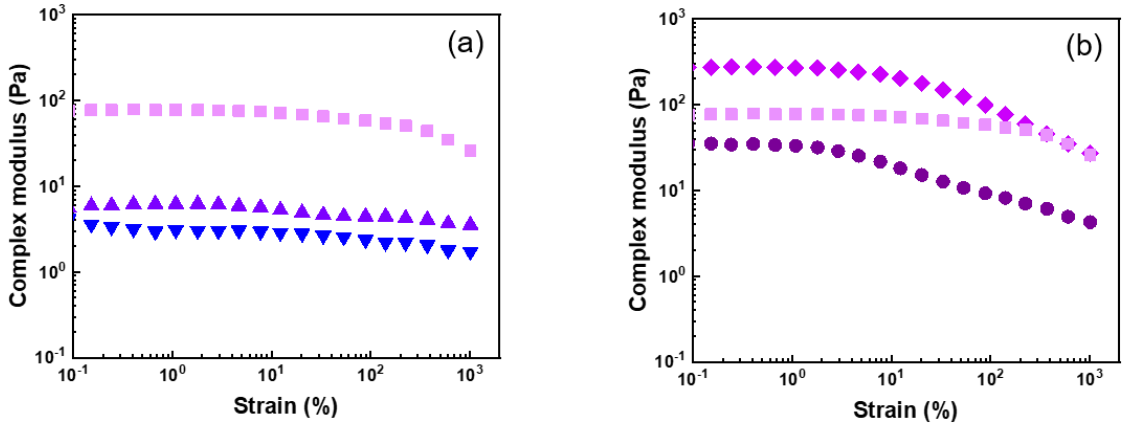

Figure S9. Complex modulus (G*) as a function of strain for PS@PMA suspensions at 10 wt% in anisole. (a) (▼) $PS_h@PMA_{20k}$, (▲) $PS_h@PMA_{30k}$ and (■) $PS_h@PMA_{40k}$ and (b) (●) $PS_l@PMA_{40k}$, (◆) $PS_m@PMA_{40k}$ and (■) $PS_h@PMA_{40k}$.

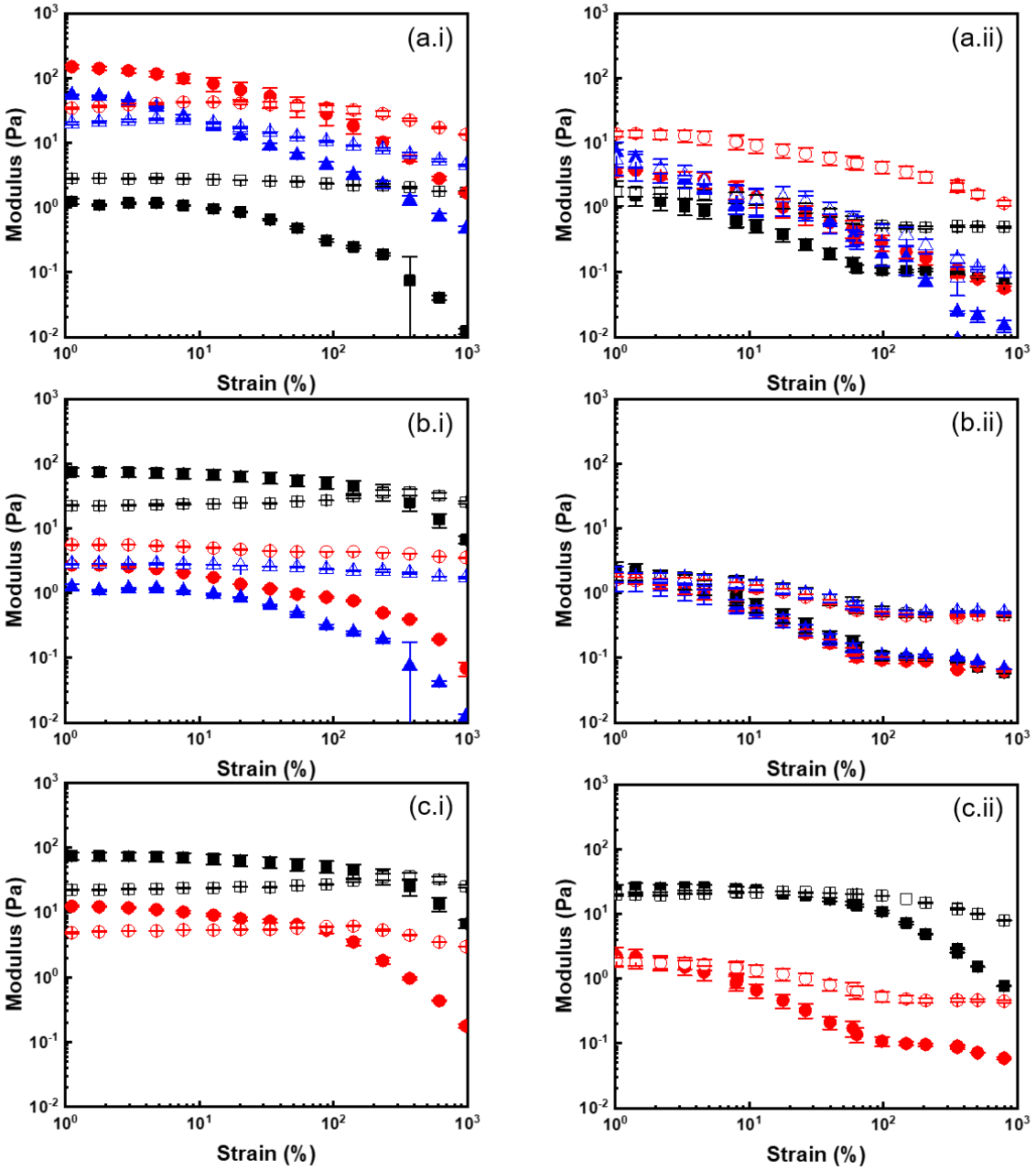

Figure S10. Elastic (close) and viscous (open) modulus of PS@PMA suspension in (i) anisole and (ii) DMSO. (a) Effect of the grafting density on 10 wt% suspension of (■) PS_h@PMA_{20k}, (●) PS_m@PMA_{20k} and (▲) PS_l@PMA_{20k}. (b) Effect of the brush length on 10 wt% suspension of (■) PS_h@PMA_{40k}, (●) PS_h@PMA_{30k} and (▲) PS_h@PMA_{20k}. (c) Effect of nanoparticle concentration in suspension of PS_h@PMA_{40k} in anisole at (■) 10 wt% (ϕ_{cal} = 0.62) and (●) 4.5 wt% (ϕ_{cal} = 0.27) and in DMSO at (■) 19 wt% (ϕ_{cal} = 0.50) and (●) 10 wt% (ϕ_{cal} = 0.25).

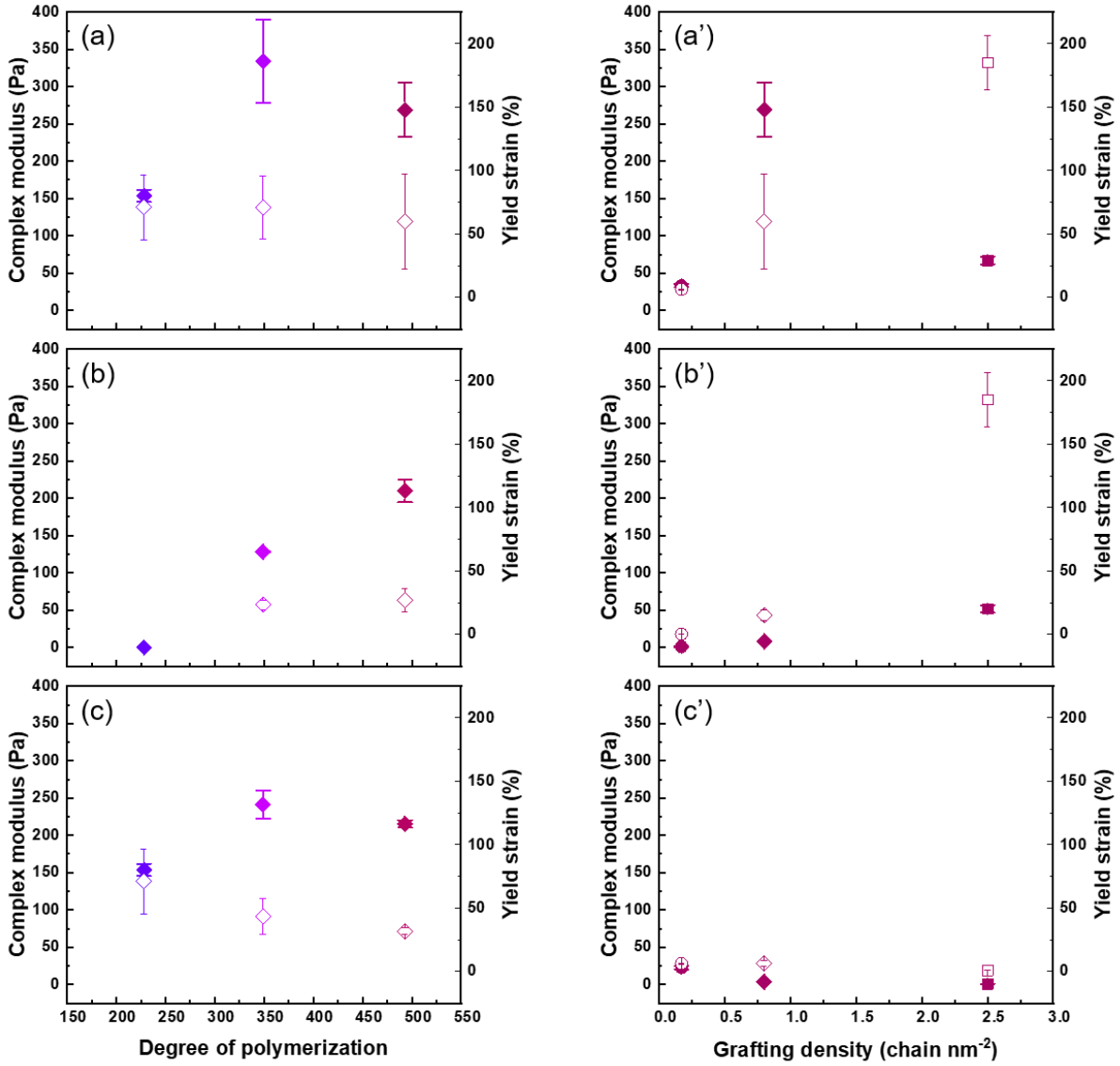

Figure S11. Effect of the architecture of the PMA canopy on the stiffness (closed symbol) and the strength (open symbol) of the colloidal gels formed with (◆) PS_m@PMA_{20k}, (◆) PS_m@PMA_{30k} and (◆) PS_m@PMA_{40k} , (■) PS_h@PMA_{40k} and (●) PS_l@PMA_{40k}. For suspension with constant weight fraction (a, a'), molar concentration of NPs (b, b') and constant concentration of methyl acrylate units (c, c').

References

1. R. W. Graff, X. Wang and H. Gao, *Macromolecules*, 2015, **48**, 2118-2126.
2. J. Brandrup, E. H. Immergut and E. A. Grulke, *Polymer Handbook*, Wiley, 4th edn., 2003.
3. I. M. Krieger and T. J. Dougherty, *Trans. Soc. Rheol.*, 1959, **3**, 137-152.